Supplementary information

Content

Supplementary methods

Cell culture

Mouse L1210 lymphocytic leukemia cells (ATCC CCL219) were grown in CO2-independent L-15 medium supplemented with 2 gr/L dextrose and 10% fetal bovine serum, penicillin G and streptomycin sulfate.

Baby machine based synchronization

Newborn cells were isolated from the baby machine device as previously described[1]. Briefly, after the apparatus that contains the funnel, a 0.22 μm pore size nitrocellulose membrane, gaskets and a ring was prepared, the membrane was rinsed with a solution of concavalin A (20 μg/ml) to allow the attachment of the cells to it, and residual conA was washed by PBS (100ml). A culture of L1210 cells ($6*10^7$) pulse labeled with 1μM BrdU for 45 min was poured on top of the filter, and the medium was drawn through by vacuum at about 1 ml/s. The filter holder was then inverted and placed on top of a second plastic funnel resting on a ring stand and connected to a peristaltic pump. The medium was pumped at a rate of 15 ml/min for the first 2 min to remove loosely attached cells and 2 ml/min thereafter. The entire procedure was performed in a 37°C incubator. Samples were collected every 45 minutes after a lag of 1 hour and 30 minutes. Synchronization of the cells isolated from the "baby machine" was assessed using a ZB Coulter electronic particle counter and flow cytometry (Figure S15). BrdU incorporation was assessed using a quantitative dot

blotting method [2] (Figure S16). Based on this analysis we excluded sample 8 from further experiments since it contained minimal amounts of BrdU.

Newly replicated DNA immunoprecipitation

Immunoprecipitation of BrdU-labeled DNA was carried out as described[3] with some modifications. DNA from each fraction was extracted, sonicated (2 cycles for 15 s) to generate fragments of an average size of 700 bp and heat denatured (3 min at 95^0c). Immunoprecipitation was performed in a 10mM sodium phosphate (pH 7.0) 0.14 M NaCl, 0.05% Triton X-100 buffer using 2µg of anti-BrdU monoclonal antibody (347580, Becton-Dickinson) at room temperature for 30 min with constant end over end rotation. Antibody-bound BrdU DNA was precipitated by addition of 20ul Protein A/G Plus Agarose beads (Santa Cruz) and incubated at 4^0c for 1 hour with constant rotation. Samples were washed in Lysis buffer (1M NaCl, 10mM EDTA,50mM Tris-HCl (pH 8.0), 0.5%SDS) two times, then in wash buffer (10 mM Tris-HCl pH 8.0, 250 mM LiCl, 0.5% NP40, 0.5% Na-deoxycholate, 1 mM EDTA) two times and lastly with TE. Pellets were resuspended in 200 µl elution buffer (50 mM Tris-HCI (pH 8.0), 10 mM EDTA, 0.5%SDS, 0.25 mg/ml proteinase K) and incubated overnight at 37^0c. An additional 100 µl of the same elution buffer was added, and samples were incubated 1 hr at 50^0c. 20µg of Glycogen was added, and the samples were extracted with phenol and chloroform and ethanol precipitated. The immunoprecipitated BrdU containing DNA was dissolved in 100 ul of Tris-HCl (pH 8.0) and stored in a dark box at -20^0c. The specificity of the immunoprecipitation was assessed by mixing BrdU labeled mouse DNA with 6 fold excess of unlabeled human DNA. The relative amounts of mouse and human DNA were measured by semi quantitative PCR using species specific primers after immunoprecipitation. Almost no human DNA was detected after the immunoprecipitation (Figure S17).

Fluorescence *in situ* hybridization

ToR of selected regions was determined by performing FISH as described [4, 5]. Briefly, BAC DNA (purchased from BACPAC Resources Center in the CHORI) was labeled, mixed with 10µg of cot-I DNA (Life Technologies) and 10µg of mouse sonicated DNA and hybridized to L1210 nuclei. ToR was determined by the percentage of S phase nuclei with single/single, single/double and double/double patterns. The percentage was determined by counting at least 100 S phase nuclei for each probe.

BAC clones used in the FISH experiments:

BAC clone	**Close to gene, region**
RP23-340N9	crisp1
RP23-352F10	adcy8
RP23-191C6	a2m
RP24-338L20	Chr16, 91.8M
RP24-65P6	Vax2
RP23-184H10	Mark1
RP23-97O1	actb
RP23-385F15	Chr16, 88.3M
RP24-122F10	Atm
RP24-267F8	Calmbp1/F13b
RP24-85E12	Psp
RP23-56C10	Mgat5

Replication fork direction determination

Replication fork direction was determined by using the protein synthesis inhibitor, emetine, which selectively inhibits lagging strand replication as described [6]. Briefly, L1210 cells were pulse labeled for 24 hours with 10uM BrdU and 2uM Emetine. BrdU-DNA was isolated by immunoprecipitation as described above. Strand specific DNA was amplified by 20 cycles of linear PCR (using a single primer) and the relative amount of the two strands was determined by semi quantitative PCR.

PCR amplification of replicated DNA

The sequences (5'->3') and the predicted product sizes of the primers used for PCR amplification are listed :

Name	**Forward sequence**	**Reverse Sequence**	**Product size**
Beta -globin	TGTGGGAAGATGGAAGAACC	TATCAGCTTCCCCTCCTCCT	383bp
Beta-actin	TCGAGCCATAAAAGGCAACT	CCATCGCCAAAACTCTTCAT	
X141 *	CATACTGACACTTGATGTCA	TCAGCTAGGATCACTGACAA	330bp
Mito DNA **	GACATCTGGTTCTTACTTCA	GTTTTTGGGGTTTGGCATTA	180bp
Chr16-A	CAATCTGTGTGGCAATTTGG	CCCAGAGGAGAGCAATGAAG	190bp
Chr16-B	TGCAGTGTTGATTGGCTAGG	GCACATGTTGTCAGGAGTGG	199bp
Chr16-C	CACAGTTCCCATGACAAACG	CCGAGGATTCTGTGTGGAGT	127bp
Chr16-D	GACTGCAAGGGGACAATGTT	TGTGGCTATGTCTGGCTGAG	105bp
Chr1-40.372M[$]	GGTCCTGGAAGGTGACAGAA	GTACCTGGGAACAGCCAGAA	120bp
Chr1-40.379M[$]	AGTGGGCTGGGTTCTTACCT	GCCAGGCAGGTCTTAGAGTG	171bp
Chr1-40.381M[$]	GCCCTGTAGAATCCCCTCTC	TACATGGGATCCACCAACCT	215bp
Chr1-40.538M[$]	CCTGCCCAGCTGTGTATAAT	GTTCAATGCATGGGACAGTG	185bp
Chr1-40.736M[$]	CCATTGTAAGCCTTGTGCCTA	CCCTCAGACTGCTGGTCTTC	151bp
Chr1-40.859M[$]	CTCCTCAGGTTGCTTTTTGC	GTACAACGTGGGGAGAGGAA	210bp
Chr1-41.07M[$]	AGGCCAACATGACTTCAACC	GCCTCAACATCCCAGACAAT	156bp
Chr1-42.28M[$]	TCTGGGATAGGCAAGGAATG	CTGTGACTGCCTCTCACCAA	237bp
Chr1-156.94M[$]	ACCTGTCTGTCCCATTTTGC	AATGGCCCCTTCTGTTCTTT	157bp
Chr1-156.97M[$]	GTTGCAAGGGCTCTGTCTTC	GGCACTGAGAGGTCCAAGAG	178bp
Chr1-157.3M[$]	TCTTGCTATCGCTCCGTTTT	CAAGAGCATCCAATGCAGAA	168bp
Chr1-173.83M[$]	CATAAAGCCTGGAGGCTCAC	ATAGACACCCACTGCCATGA	197bp
Chr1-173.85M[$]	GGCTGGATCAGTCCAT	TCACAGTGCACCTTCC	238bp
Chr1-174.3M[$]	TAGCACACAGCACCTTCCAG	GTACCAGGGCAGGACAGAAA	178bp
Chr1-174.4M[$]	CCTTCACTGAGTTCCCTTCG	GAAGCTGTTCCTCCATGCTC	168bp
Chr8-108.2M[$]	TCCCGGTTGCTAGAAGCTAA	TGTACTCTGCCATGCTCAGG	185bp
Chr8-108.4M[$]	TTTAGGGCCGTGTTAAGGTG	TTATGCGCTCTGACAGGATG	194bp
Chr8-108.7M[$]	AACAGTCACCCTGTCCCAAG	TCTGTGCCTGGATCTCTGTG	241bp

* Mileham and Brown, Mammalian genome 7, 253-256, 1996.
** *Alla Buzina et al., NAR 33, 4412-4424, 2005.*
[$] *based on mm6 assembly.*

PCR amplifications (30-32 cycles) included 0.125ul of Titanium Taq Polymerase (Clontech) and 2µl of antibody purified BrdU-labelled DNA or amplified BrdU-labeled DNA as a template (amplification didn't change the purified BrdU-labeled DNA content, data not shown) in 25µl standard reaction buffer .

X141 PCR reaction contained 1µM primers, all other reactions contained 0.5µM primers. PCR products were separated by electrophoresis on 2% agarose gels.

For replication fork direction determination the semiquantitative PCR was carried on the results of linear PCR reaction performed with a single primer. The linear amplification step allowed the specific amplification of a single strand and thus

retains the information about the differences in the abundance of the two strands. The linear amplification was carried out by performing 15-20 cycles of PCR with a single primer (either reverse or forward). The annealing temperature in those reactions was 65°C.

Amplification of DNA

Amplification of DNA for microarray hybridization was carried out as described[7] with some modifications. Briefly, in Round A, two rounds of DNA synthesis were performed using a partially degenerate primer (Primer A GTTTCCCAGTCACGATCNNNNNNNNN), T7 sequenase and slow ramp times. Primer A concentration was calibrated to work best in 200uM. In Round B, 17-21 cycles of PCR were carried out using a primer (primer B GTTTCCCAGTCACGATC) that anneals to a specific region of primerA and unlabeled dNTPs. Samples were then cleaned in QIAGEN PCR purification kit and the amount of DNA was measured using a nano-drop device.

Labeling of DNA Hybridization to the Agilent mouse CGH microarrays

Labeling and Hybridization was carried out according to Agilent's CGH protocol (*www.embl-heidelberg.de/courses/Agilent05/CGH-Protocol.pdf*). Briefly, 5ug from each sample were labeled using the BioPrime Array CGH Genomic Labeling Module. Reference samples were labeled in Cyanine 3-dUTP, and samples from the time course were labeled in Cyanine 5-dUTP. Hybridization was performed on Agilent mouse CGH 44k microarrays.

PolII ChIP on chip analysis

ChIP on chip was carried out as described[8]. Briefly, L1210 cells are fixed with 1% formaldehyde for 20 minutes at room temperature, harvested and rinsed with 1x PBS. The resultant cell pellet is sonicated, and DNA fragments that are crosslinked to a protein of interest are enriched by immunoprecipitation with 10µg of RNA polymerase II-specific antibody (8WG16 MMS-126R, COVANCE). After reversal of the crosslinking, both IP-enriched and unenriched DNA are amplified using ligation-mediated PCR (LM-PCR). 100ng of the amplified DNA is labeled with aminoalyl-dUTP, using high concentration Klenow polymerase, which is then coupled to one of two Cyanine dyes (Cy3 or Cy5), essentially as described[9] . Both IP-enriched and unenriched pools of labeled DNA are hybridized to a single DNA microarray containing 13,000 mouse intergenic regions (Mouse promoterChip BCBC-5A purchased from beta cell consortium). The ChIP on chip data were mode normalized and the average log ratios of two biological replicates was calculated. Genes were included in the set of 'bound' genes if the enrichment (average $\log_2$ ratio) was at least 0.5 (FDR=0.1).

Dot-Blot analysis

Dot-blot analysis was carried out as described[2]. Briefly, concentration of BrdU-labeled DNA from each fraction was measured using the nano-drop device. The DNA (2 µg) was denatured by incubation with 10 volumes of 0.4 N NaOH solution for 30 min at room temperature and kept on ice to prevent annealing. The DNA solution was placed on ice and neutralized by an equal volume of 1M Tris·HCl (pH 6.8). Equal amounts of DNA (50 ng in 5 µl) was dot-blotted onto a nitrocellulose membrane (Schleicher & Schuell) and fixed by ultraviolet cross-linker Stratalinker (Stratagene). To visualize the BrdU signal, detection methods similar to Western blot analysis were

performed. Briefly, the membrane was incubated with mouse anti-BrdU monoclonal antibody (1:2,000 dilution, Becton-Dickinson) in TBST buffer (20 mM Tris·HCl, pH 7.6, 136 mM NaCl, and 0.05% Tween 20) containing 1% nonfat milk for 1 h at room temperature. After being washed with TBST (10 min x 3 times at room temperature), the membrane was incubated with a horseradish peroxidase-conjugated anti-mouse IgG antibody (1:5,000 dilution, Upstate) for 1 h at room temperature. The membrane was washed with TBST 3 times, analyzed by enhanced chemiluminescence and exposed to autoradiography film (FujiFilm).

Bioinformatics analysis

Autocorrelation was calculated with the ACF function in matlab. The GC content for each probe was calculated for the 20Kbp region surrounding the probe. Tissue specificity index in mouse was kindly provided by Dr. Itai Yanai, based on [10]. Expression data was downloaded from the GNF [11]. The conservation between human and mouse ToR was determined by locating the human homolog of a mouse gene (as defined by the DBTSS database (*http://dbtss_old.hgc.jp/hg17/*) in the human BAC clones used in [12]. GO analysis was carried out using STEM [13], with randomization as a multiple hypothesis correction. Significance of enrichments was calculated using the hypergeometric p-value unless stated otherwise.

Name	Cluster	Reported replication timing	reference	remarks
Rag-1	IV	E	3	
CD8	II	E	3	
TdT	II	E	3	
-Globin	I	E	14	
C9	I	E	14	
Thy-1	I	E	14	
Tyrosine amino-	II	E	14	
Metallothionein	I	E	14	
Afp	V	L	14	
Albumin	V	L	14	
-globin	VI	L	14	
CD19	I	E	3	
CD11	I	E	3	
Foxd10	IV	M	15	
Nanog	I	E	15	
C/EBPalpha	I	ME	15	E in ES and HSC cells
c-myb	I	E	15	
Gata1	I	E	15	
Gata9	I	E	15	
Gata10	IV	E	15	ME in HSC
Lmo9	I	E	15	
Pax5	I	ME	15	E in ES cells
Myf5	I	L	15	
MyoD	I	E	15	
Myog	I	E	15	
Hes1	I	E	15	
Hes5	I	E	15	
Irx10	IV	M	15	
Mash1	IV	L	15	ML in HSC cells
Msx1	IV	L	15	ML in HSC cells, ME in ES cells
Ngn1	II	E	15	
Ngn9	II	ME	15	
Nkx9-9	IV	M	15	
Nkx9-9	V	L	15	
Olig9	I	E	15	
Pax10	V	L	15	
Pax6	IV	M	15	
Pax7	I	ME	15	E in ES cells
Sox10	VI	L	15	
Dmrt1	I	E	16	
Tdgf1 / Cripto	I	E	16,15	
Tcfap9c	II	E	16	
Utf1	II	E	16,15	
90100011A010Rik	I	E	16	
Ptgis	I	E	16	
Epha9	I	E	16	
Pcolce	I	E	16	
Ltbr	I	E	16	
Ddr1	I	E	16	
Dll1	I	E	16	
Mmp15	I	E	16	
Slc95a10	I	E	16	
Nfatc1	I	E	16	
Cdh11	I	E	16	
Bmp1	I	E	16	
Fgfr1	I	E	16	
Gpr56	I	E	16	
Cspg10	I	E	16	
Lmo1	V	E	16	
Ptn	VI	L	16	
Tm11sf19	V	L	16	
Ptprz1	V	L	16	
Postn	IV	L	16	
Lox	V	L	16	
Sox6	IV	E	16	
Ptgs9	V	L	16	
Crisp1	V	E	16	validated in FISH to be L
Adcy8	V	E	16	validated in FISH to be L
Spp1	V	E	16	
Car8	V	E	16	
Nr0b1	V	L	16	
A9m	III	L	16	validated in FISH to be M
170001011H111Rik	IV	E	16	
Ddx11	II	E	16	
Rbpms	I	E	16	
Tfpi	I	E	16	
Mme	V	E	16	
Egfr	V	E	16	
Col1a9	VI	E	16	
Terf1	IV	E	16	
C1qr1	V	L	16	

Table S1 - comparison with the literature

In order to confirm our replication timing assignments, we performed a literature search and compiled previous information about the time of replication of mouse genes. The table contains the literature information along with the time of replication assigned by us. The colors mark cases in which our data confirm previous knowledge in a similar tissue (light blue; 60/81=74%), or only in a different tissue (yellow; additional 6 genes - 7.4%; the tissue in which the published TOR correspond to the microarray data is stated in the remarks column). Three of the cases in which our data contradict previous assignments were experimentally examined by us using the FISH procedure and in all those cases (labeled in purple) our assignment was confirmed. Overall 85% of the cases fit our assignments. In references3,14 and 15 replication timing were measured in lymphocytes whereas in reference 16 replication timing was measured in embryonic stem cells.

Replication time zone	Category ID	Category Name	#Genes Category	#Genes Assigned	#Genes Expected	#Genes Enriched	p-value	Corrected p-value
I	GO:0050875	cellular physiological process	6068	3113	2487.1	625.9	6.80E-81	<0.001
I	GO:0044238	primary metabolism	4131	2171	1693.1	477.9	3.70E-62	<0.001
I	GO:0008152	metabolism	4613	2383	1890.7	492.3	8.20E-61	<0.001
I	GO:0044237	cellular metabolism	4265	2202	1748.1	453.9	5.10E-55	<0.001
I	GO:0043170	macromolecule metabolism	2503	1366	1025.9	340.1	5.00E-48	<0.001
I	GO:0019538	protein metabolism	1874	1025	768.1	256.9	5.90E-36	<0.001
I	GO:0044267	cellular protein metabolism	1769	974	725	249	1.40E-35	<0.001
I	GO:0044260	cellular macromolecule metabolism	1800	982	737.8	244.2	7.90E-34	<0.001
I	GO:0043283	biopolymer metabolism	1532	842	627.9	214.1	2.50E-30	<0.001
I	GO:0006139	nucleobase, nucleoside, nucleotide and nucleic a	1911	987	783.2	203.8	5.50E-23	<0.001
I	GO:0006464	protein modification	976	547	400	147	2.50E-22	<0.001
I	GO:0051244	regulation of cellular physiological process	1863	961	763.6	197.4	3.70E-22	<0.001
I	GO:0043412	biopolymer modification	1011	562	414.4	147.6	7.70E-22	<0.001
I	GO:0050794	regulation of cellular process	2019	1030	827.5	202.5	9.90E-22	<0.001
I	GO:0050791	regulation of physiological process	1940	992	795.1	196.9	2.50E-21	<0.001
I	GO:0044249	cellular biosynthesis	682	390	279.5	110.5	3.80E-18	<0.001
I	GO:0009058	biosynthesis	773	428	316.8	111.2	1.70E-16	<0.001
I	GO:0019222	regulation of metabolism	1460	748	598.4	149.6	2.00E-16	<0.001
I	GO:0009059	macromolecule biosynthesis	430	257	176.2	80.8	1.90E-15	<0.001
I	GO:0031323	regulation of cellular metabolism	1397	714	572.6	141.4	2.00E-15	<0.001
I	GO:0006810	transport	1758	877	720.5	156.5	2.60E-15	<0.001
I	GO:0006350	transcription	1324	676	542.7	133.3	1.60E-14	<0.001
I	GO:0006412	protein biosynthesis	388	233	159	74	1.90E-14	<0.001
I	GO:0016043	cell organization and biogenesis	995	524	407.8	116.2	2.00E-14	<0.001
I	GO:0051179	localization	1968	961	806.6	154.4	1.10E-13	<0.001
I	GO:0019219	regulation of nucleobase, nucleoside, nucleotide	1302	661	533.6	127.4	1.40E-13	<0.001
I	GO:0051234	establishment of localization	1953	953	800.5	152.5	1.80E-13	<0.001
I	GO:0045449	regulation of transcription	1286	651	527.1	123.9	4.30E-13	<0.001
I	GO:0007242	intracellular signaling cascade	615	336	252.1	83.9	3.20E-12	<0.001
I	GO:0006351	transcription, DNA-dependent	1220	615	500	115	5.30E-12	<0.001
I	GO:0006355	regulation of transcription, DNA-dependent	1205	607	493.9	113.1	8.60E-12	<0.001
I	GO:0006996	organelle organization and biogenesis	477	267	195.5	71.5	1.90E-11	<0.001
I	GO:0006793	phosphorus metabolism	562	303	230.3	72.7	2.70E-10	<0.001
I	GO:0006796	phosphate metabolism	562	303	230.3	72.7	2.70E-10	<0.001
I	GO:0050790	regulation of catalytic activity	126	84	51.6	32.4	4.80E-09	<0.001
I	GO:0008104	protein localization	413	226	169.3	56.7	9.40E-09	<0.001
I	GO:0016310	phosphorylation	462	248	189.4	58.6	1.80E-08	<0.001
I	GO:0045184	establishment of protein localization	395	214	161.9	52.1	6.60E-08	<0.001
I	GO:0051243	negative regulation of cellular physiological proce	389	211	159.4	51.6	7.20E-08	<0.001
I	GO:0015031	protein transport	379	206	155.3	50.7	8.30E-08	<0.001
I	GO:0009607	response to biotic stimulus	449	239	184	55	8.40E-08	<0.001
I	GO:0006955	immune response	372	202	152.5	49.5	1.20E-07	<0.001
I	GO:0007049	cell cycle	358	195	146.7	48.3	1.50E-07	<0.001
I	GO:0016070	RNA metabolism	250	143	102.5	40.5	1.50E-07	<0.001
I	GO:0043118	negative regulation of physiological process	407	218	166.8	51.2	1.60E-07	<0.001
I	GO:0006915	apoptosis	346	189	141.8	47.2	1.80E-07	<0.001
I	GO:0051649	establishment of cellular localization	393	211	161.1	49.9	2.00E-07	<0.001
I	GO:0006512	ubiquitin cycle	258	146	105.7	40.3	2.70E-07	<0.001
I	GO:0046907	intracellular transport	390	209	159.8	49.2	2.80E-07	<0.001
I	GO:0051641	cellular localization	399	213	163.5	49.5	3.10E-07	<0.001
I	GO:0006950	response to stress	526	272	215.6	56.4	3.30E-07	<0.001
I	GO:0006952	defense response	426	225	174.6	50.4	4.40E-07	<0.001
I	GO:0012501	programmed cell death	352	190	144.3	45.7	5.00E-07	<0.001
I	GO:0006468	protein amino acid phosphorylation	406	215	166.4	48.6	6.10E-07	<0.001
I	GO:0048519	negative regulation of biological process	499	258	204.5	53.5	6.70E-07	<0.001
I	GO:0007243	protein kinase cascade	136	84	55.7	28.3	7.70E-07	<0.001
I	GO:0016265	death	369	197	151.2	45.8	8.50E-07	<0.001
I	GO:0008219	cell death	369	197	151.2	45.8	8.50E-07	<0.001
I	GO:0048523	negative regulation of cellular process	461	239	188.9	50.1	1.30E-06	<0.001
I	GO:0043285	biopolymer catabolism	153	92	62.7	29.3	1.30E-06	<0.001
I	GO:0042981	regulation of apoptosis	222	126	91	35	1.40E-06	<0.001
I	GO:0006457	protein folding	113	71	46.3	24.7	2.20E-06	<0.001
I	GO:0009057	macromolecule catabolism	201	115	82.4	32.6	2.30E-06	<0.001
I	GO:0006396	RNA processing	191	110	78.3	31.7	2.50E-06	<0.001
I	GO:0005975	carbohydrate metabolism	297	161	121.7	39.3	2.50E-06	<0.001
I	GO:0043067	regulation of programmed cell death	226	127	92.6	34.4	2.60E-06	<0.001
I	GO:0006886	intracellular protein transport	259	142	106.2	35.8	4.30E-06	0.004
I	GO:0006807	nitrogen compound metabolism	228	127	93.4	33.6	4.70E-06	0.004
I	GO:0019752	carboxylic acid metabolism	303	162	124.2	37.8	6.90E-06	0.004
I	GO:0006082	organic acid metabolism	303	162	124.2	37.8	6.90E-06	0.004
I	GO:0006259	DNA metabolism	301	161	123.4	37.6	7.10E-06	0.004
I	GO:0030163	protein catabolism	130	78	53.3	24.7	9.10E-06	0.004
I	GO:0007028	cytoplasm organization and biogenesis	61	42	25	17	9.90E-06	0.006
I	GO:0046649	lymphocyte activation	93	59	38.1	20.9	1.00E-05	0.006
I	GO:0045321	immune cell activation	107	66	43.9	22.1	1.20E-05	0.006
I	GO:0009308	amine metabolism	216	119	88.5	30.5	1.80E-05	0.006
I	GO:0051603	proteolysis during cellular protein catabolism	108	66	44.3	21.7	1.90E-05	0.006
I	GO:0001775	cell activation	108	66	44.3	21.7	1.90E-05	0.006
I	GO:0044257	cellular protein catabolism	108	66	44.3	21.7	1.90E-05	0.006
I	GO:0043037	translation	112	68	45.9	22.1	1.90E-05	0.006
I	GO:0048518	positive regulation of biological process	453	229	185.7	43.3	2.10E-05	0.006
I	GO:0051726	regulation of cell cycle	190	106	77.9	28.1	2.50E-05	0.006
I	GO:0009056	catabolism	356	184	145.9	38.1	2.60E-05	0.006
I	GO:0051246	regulation of protein metabolism	151	87	61.9	25.1	2.60E-05	0.006
I	GO:0042110	T cell activation	59	40	24.2	15.8	2.80E-05	0.006
I	GO:0044265	cellular macromolecule catabolism	174	98	71.3	26.7	3.00E-05	0.006
I	GO:0007264	small GTPase mediated signal transduction	191	106	78.3	27.7	3.40E-05	0.008
I	GO:0000074	regulation of progression through cell cycle	189	105	77.5	27.5	3.50E-05	0.008
I	GO:0007010	cytoskeleton organization and biogenesis	229	124	93.9	30.1	3.70E-05	0.008
I	GO:0051338	regulation of transferase activity	69	45	28.3	16.7	4.10E-05	0.008
I	GO:0016568	chromatin modification	75	48	30.7	17.3	4.70E-05	0.008
I	GO:0046651	lymphocyte proliferation	40	29	16.4	12.6	5.30E-05	0.01
I	GO:0043085	positive regulation of enzyme activity	66	43	27.1	15.9	6.20E-05	0.018
I	GO:0043549	regulation of kinase activity	68	44	27.9	16.1	6.60E-05	0.018
I	GO:0009605	response to external stimulus	271	142	111.1	30.9	8.90E-05	0.034
I	GO:0009892	negative regulation of metabolism	184	101	75.4	25.6	9.20E-05	0.036
I	GO:0006954	inflammatory response	116	68	47.5	20.5	9.20E-05	0.036
I	GO:0030097	hemopoiesis	114	67	46.7	20.3	9.30E-05	0.036
I	GO:0051276	chromosome organization and biogenesis	149	84	61.1	22.9	1.00E-04	0.04
I	GO:0043086	negative regulation of enzyme activity	27	21	11.1	9.9	1.10E-04	0.04
I	GO:0009100	glycoprotein metabolism	73	46	29.9	16.1	1.20E-04	0.042
I	GO:0018193	peptidyl-amino acid modification	54	36	22.1	13.9	1.20E-04	0.042
I	GO:0006818	hydrogen transport	56	37	23	14	1.30E-04	0.044
II	GO:0001910	regulation of immune cell mediated cytotoxicity	7	5	0.6	4.4	8.30E-05	0.03
II	GO:0031341	regulation of cell killing	7	5	0.6	4.4	8.30E-05	0.03
III	GO:0045095	keratin filament	12	8	0.9	7.1	4.10E-07	0.001
III	GO:0006030	chitin metabolism	9	5	0.7	4.3	2.40E-04	0.088
IV	GO:0030901	midbrain development	11	7	1.4	5.6	1.00E-04	0.066
V	GO:0007186	G-protein coupled receptor protein signaling path	1135	255	135	120	8.5E-25	<0.001
V	GO:0007166	cell surface receptor linked signal transduction	1542	293	183.3	109.7	5.7E-17	<0.001
V	GO:0007165	signal transduction	2371	357	281.9	75.1	7.4E-07	<0.001
V	GO:0007154	cell communication	2520	368	299.6	68.4	9.3E-06	<0.001
V	GO:0007606	sensory perception of chemical stimulus	99	27	11.8	15.2	2.4E-05	0.006
VI	GO:0007186	G-protein coupled receptor protein signaling path	1135	267	100.5	166.5	2.7E-52	<0.001
VI	GO:0007166	cell surface receptor linked signal transduction	1542	286	136.5	149.5	4.6E-35	<0.001
VI	GO:0007606	sensory perception of chemical stimulus	99	40	8.8	31.2	2.5E-17	<0.001
VI	GO:0007154	cell communication	2520	339	223.1	115.9	4.8E-16	<0.001
VI	GO:0007165	signal transduction	2371	320	209.9	110.1	2.4E-15	<0.001
VI	GO:0007608	sensory perception of smell	61	28	5.4	22.6	3E-14	<0.001
VI	GO:0031424	keratinization	19	13	1.7	11.3	3.2E-10	<0.001
VI	GO:0050877	neurophysiological process	343	65	30.4	34.6	3.4E-09	<0.001
VI	GO:0007600	sensory perception	216	46	19.1	26.9	1.7E-08	<0.001
VI	GO:0009913	epidermal cell differentiation	29	13	2.6	10.4	3.5E-07	<0.001
VI	GO:0048730	epidermis morphogenesis	33	13	2.9	10.1	2.1E-06	0.002
VI	GO:0050909	sensory perception of taste	29	12	2.6	9.4	2.8E-06	0.002
VI	GO:0007214	gamma-aminobutyric acid signaling pathway	10	7	0.9	6.1	4E-06	0.004

Table S2 -GO annotation analysis

Each of the seven replication time zones was analyzed for enrichment of GO biological process categories using the STEM software. The P values were corrected for multiple hypothesis using 1000 randomizations. All categories with corrected P<0.05 are shown. House keeping categories are labeled in cyan, lymphocytes specific categories in purple, other tissue specific categories in yellow and stress and apoptosis categories in green.

a.

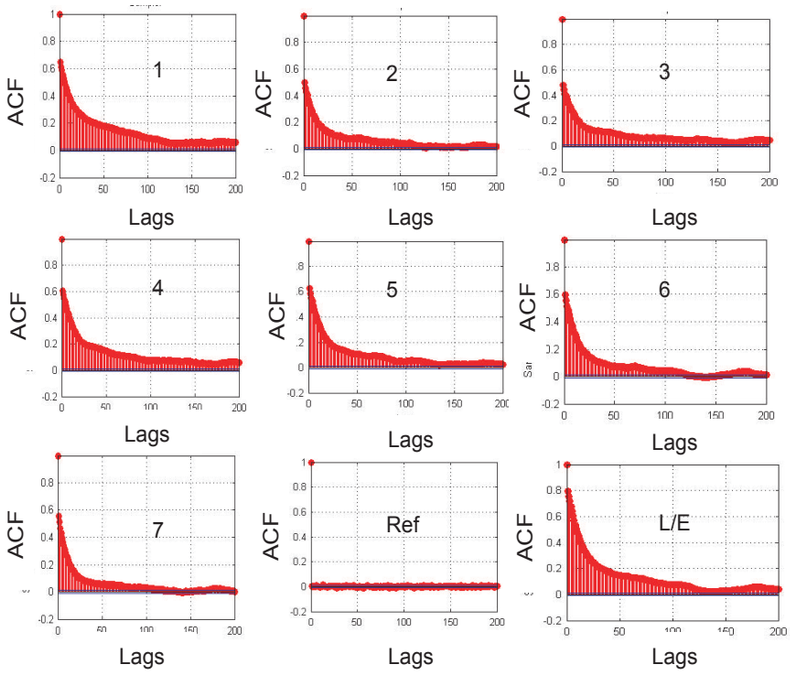

Data sorted by location on chromosome

b.

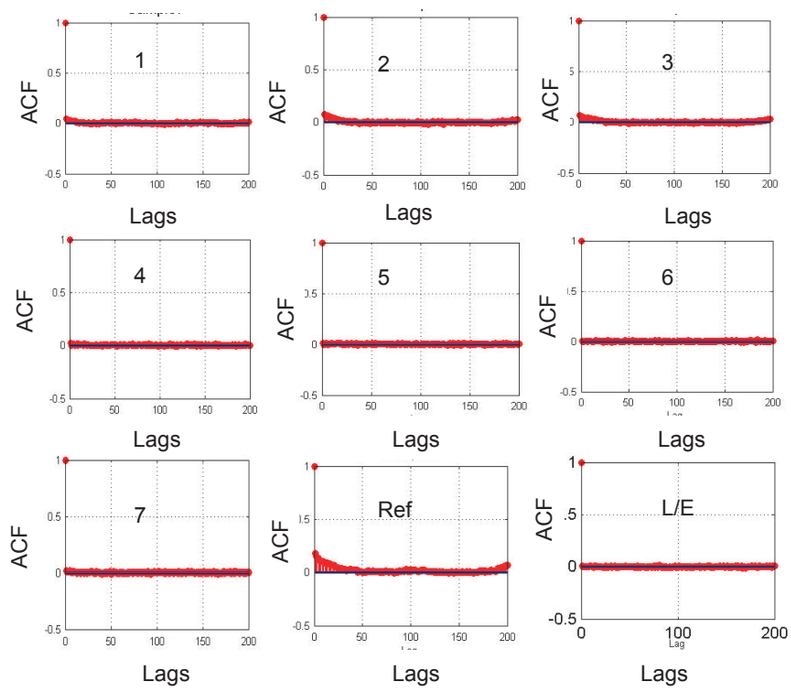

Data soretd by location on the array

Figure S1 Autocorrelation analysis
Autocorrelation of all probes for all samples with their neighboring probes sorted by their chromosomal position (a) or location on the array (b) at increasing distance (lag). Note that, in a, strong correlation is observed for up to at least 100 neighboring sequences (lag=100) for all samples besides the reference sample, whereas, in b, no significant autocorrelation is evident for the data sorted by array location.

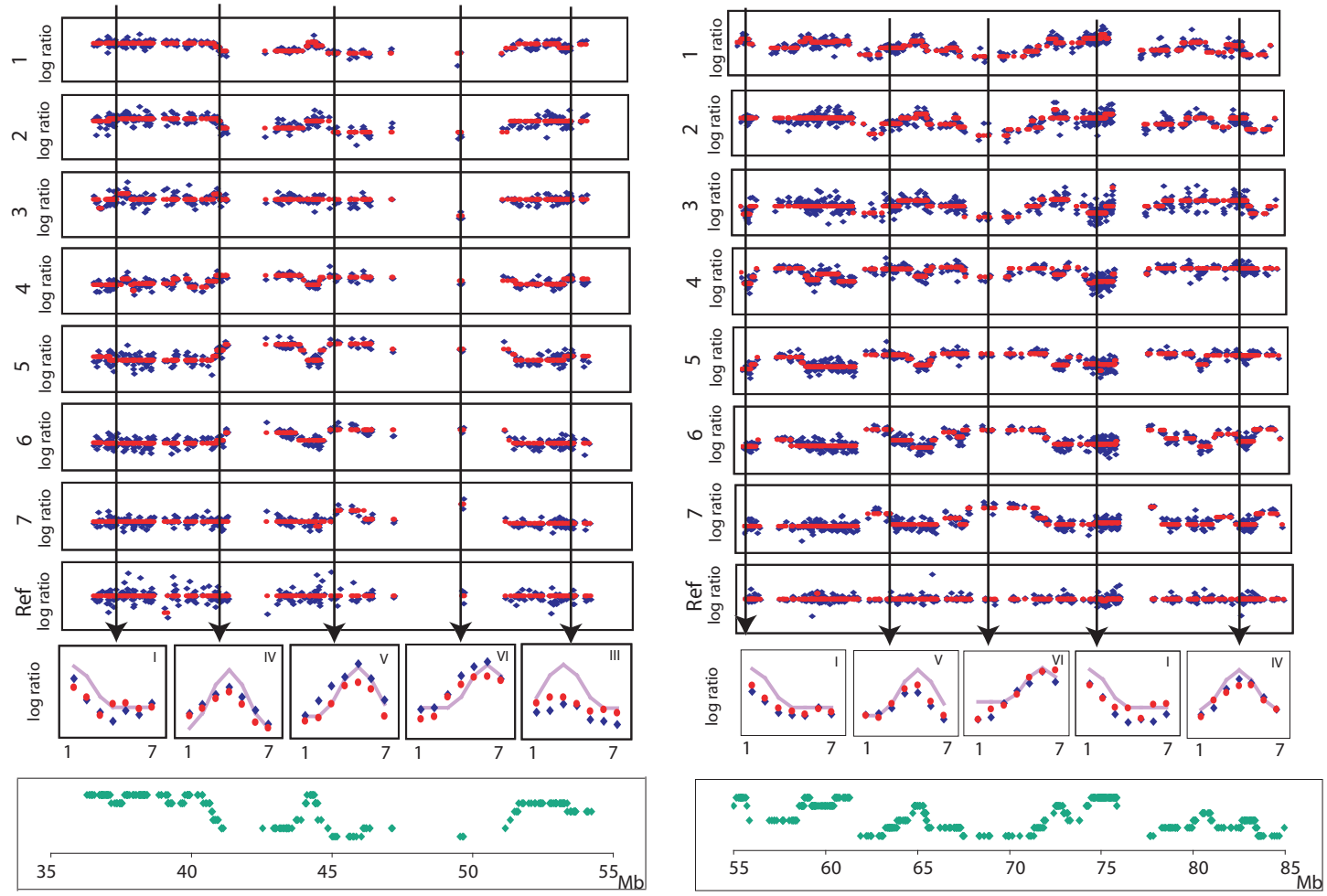

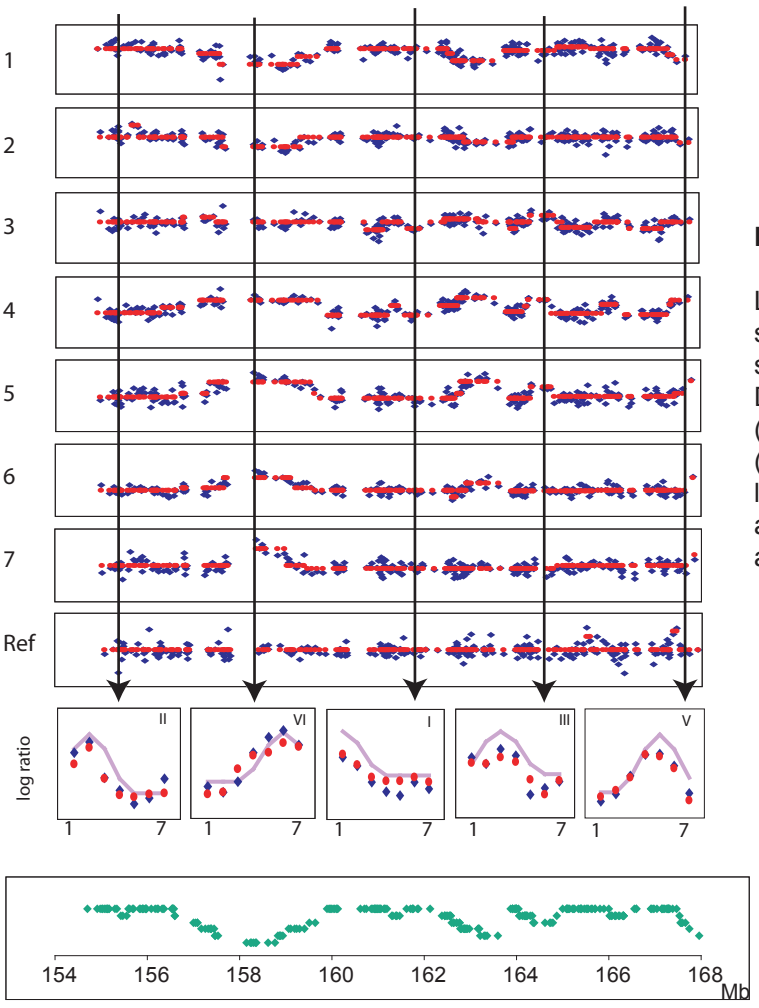

Figure S2 Genome wide measurements of replication timing.

Large genomic regions of chromosome 1 (total of 64Mb) are shown. BrdU enrichment raw (blue) and processed (red) data are shown for samples 1-7 and for the control experiments (ref). Detailed description of the raw and processed enrichment values (blue and red respectively) are shown for selected regions (arrows) along with the ToR cluster they were assigned to (purple line). The Roman numbers in each graph represent the ToR assignment (same as in figure 3a). ToR maps of the entire region are shown in the lower panels.

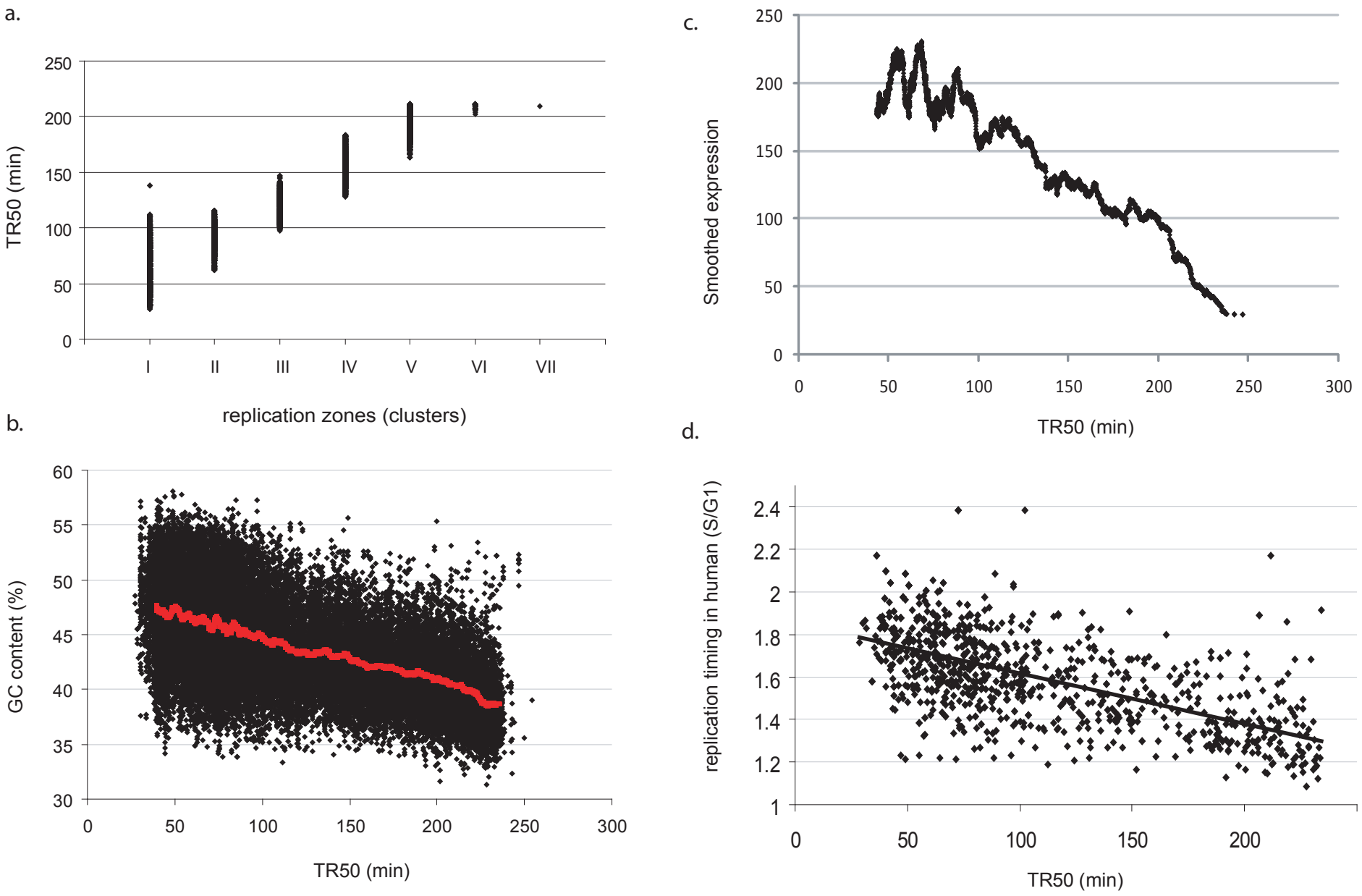

Figure S3 Comparison between two analysis methods (TR50 and supervised clustering)
a. Correlation between TR50 values and replication zones assignment for all probes in the array (r=0.95). b. Correlation between TR50 and GC content (r=0.5) , smoothed GC content (window size = 1000 probes) is overlaid in red. This analysis is equivalent to the analysis presented in Fig3b for the replication zones assignment. c. Correlation between TR50 and smoothed (window size=1000 probes) expression in L1210 cells. This analysis is equivalent to the analysis presented in FigS11 for the replication zones assignment. d. Correlation between replication timing in mouse (TR50) and human (S/G1 ratio; White et al.), linear regression is overlaid in black (r=0.61). This analysis is equivalent to the analysis presented in Fig6 for the replication zones assignment.

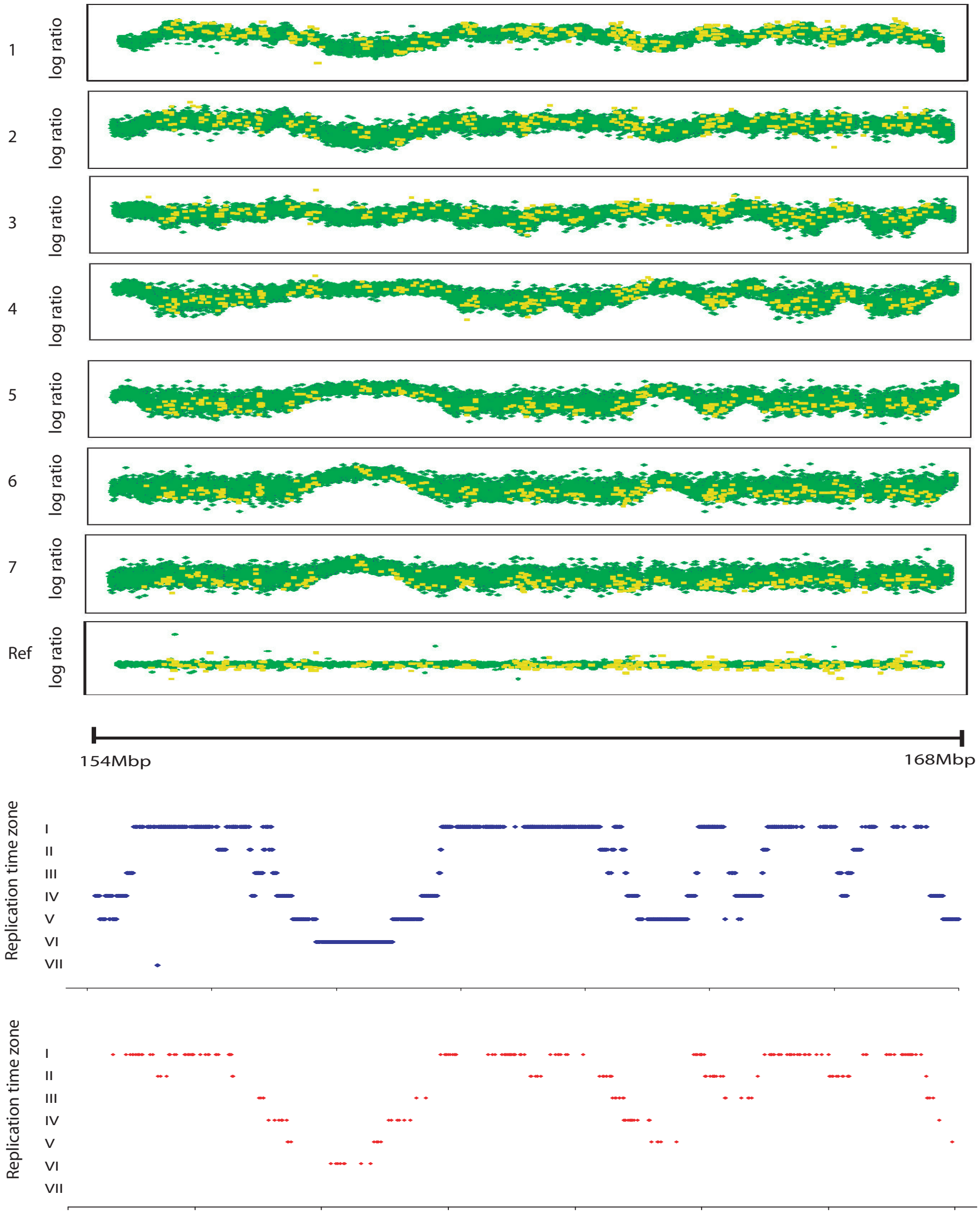

Figure S4 Comparison between high and low resolution arrays
Raw enrichment values of the seven samples and of the control experiment (Ref) from the aCGH arrays (yellow) and from a high density array with 1Kb spacing between probes (green) are overlaid one on top of the other, for 14Mb region on mouse chromosome 1. The data from both types of arrays was processed and the assigned ToR is shown in the bottom panels (blue for the tiling array and red for the aCGH). Note that the two maps are almost identical with 98% of the regions assigned a ToR identical or very similar (maximum difference of 45 minutes).

a.

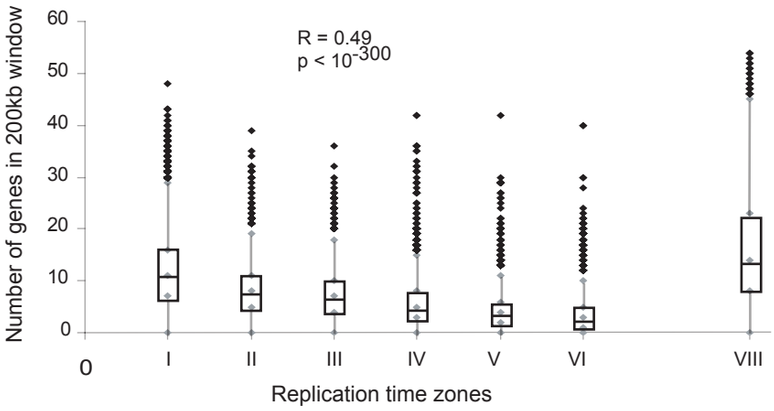

b.

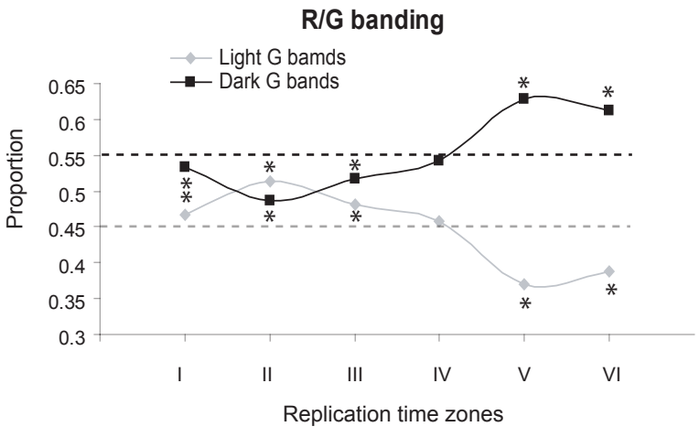

Figure S5 Gene Density and Giemsa Bands correlation to replication timing
a. Box plot representation of gene density in the 200 Kb regions surrounding each probe assigned to each cluster. The correlation to a regression line (R) and the F statistic P value are shown. Note the nice correspondence between the replication timing and the gene density and the high gene density observed for asynchronous genes (cluster VIII). b. the percentage of probes reside in light (grey) or dark (black) Giemsa bands in each of the replication time zones. The average percentage of probes in each type of bands is marked with dashed lines. Asterisks marks cases in which the observed values differ significantly (P<0.0005) from the average.

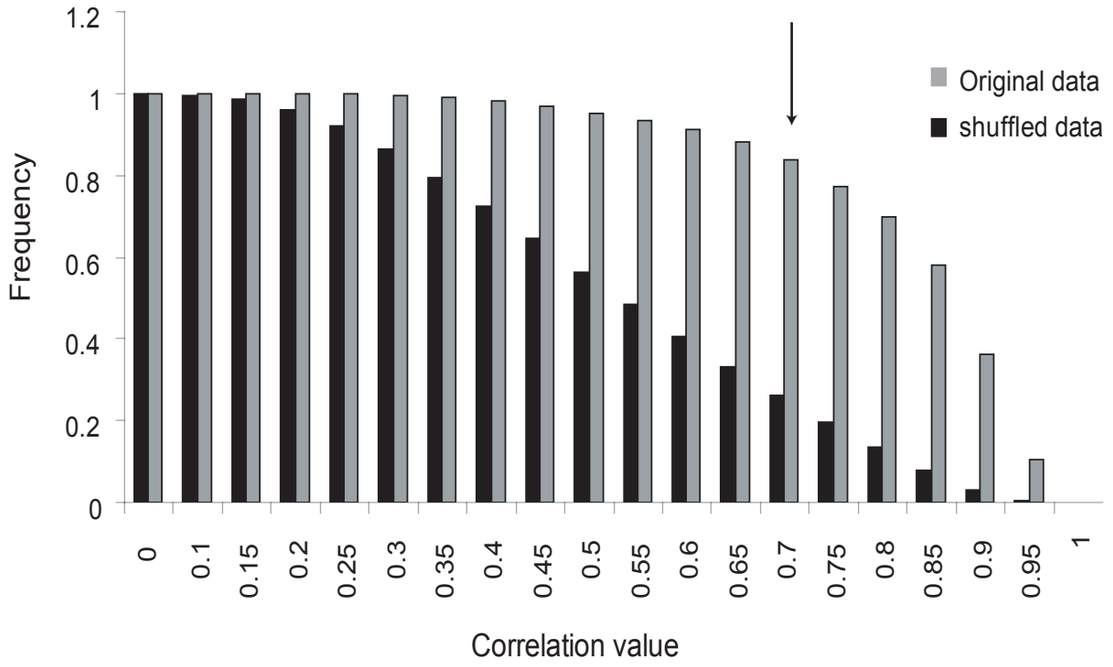

Figure S6 Effect of shuffling the data on replication timing assignment
For each probe the correlation to the seven predefined patterns (figure 3a) was calculated and the maximum value was considered. Cumulative histogram of the frequency of probes having at least a given correlation value for the original data (grey) and for shuffled data (black) is shown. The arrow marks the threshold chosen for further analysis (r<=0.7). Note that the original data show higher correlation values than the shuffled data, indicating that indeed most of the genome replicates at a discrete time. For example at the chosen threshold of r<=0.7 there is 2.8 folds enrichment over the shuffled data.

A.

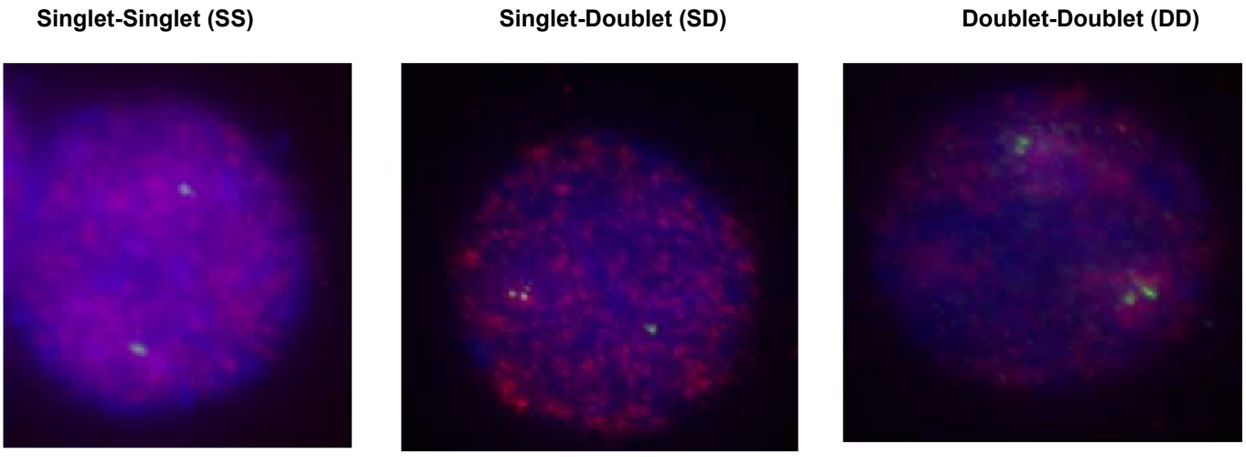

B.

replication time cluster assignment	BAC clone	SS	SD	DD
I	RP24-338L20	21.77%	7.26%	70.97%
I	RP23-97O1	15.69%	4.90%	79.41%
II	RP24-65P6	23.23%	9.09%	67.68%
III	RP23-191C6	41.84%	5.10%	53.06%
IV	RP24-267F8	50.00%	5.26%	44.74%
V	RP23-340N9	71.43%	9.82%	18.75%
V	RP23-352F10	72.95%	7.38%	19.67%
VI	RP23-385F15	68.92%	8.11%	22.97%
VIII	RP23-56C10	13.13%	33.33%	53.54%
VIII	RP23-184H10	6.70%	35.60%	57.70%
VIII	RP24-122F10	20.83%	44.79%	34.38%

Figure S7 FISH based validation of the replication timing

The time of replication of a locus can be determined by counting the percentage of S phase nuclei in which no allele replicated (singlet-singlet; SS) one allele replicated (singlet- Doublet; SD) or both alleles replicated (doublet-doublet; DD). Representative nuclei for each of these patterns are shown in A. The percentages of S phase nuclei showing each pattern for 11 BAC clones are shown in B along with the replication zone assigned in the current study for these regions. The difference between the percentage of the SD of cluster VIII probes (red) and the average SD of the other probes is extremely significant (P Value <10-40 for each; Z test), suggesting that indeed those probes replicate asynchronously.

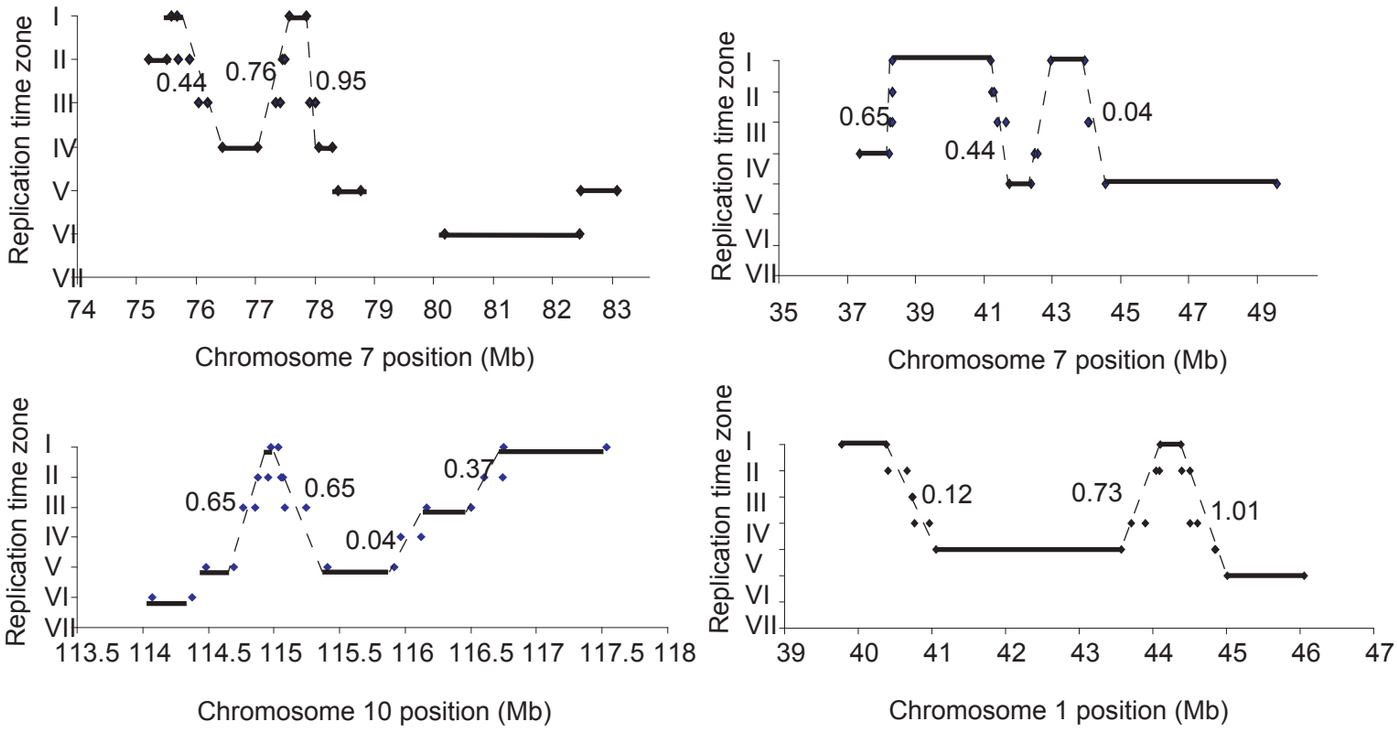

Figure S8 Genomic organization of the replication zones
Large replication segments (>250Kb; black bars) and small replication segments (<250Kb; each flanked by two dots) are shown for several regions. The vertical position of each line represents its replication time and the horizontal position its location on the different chromosomes. Dashed lines represent the predicted replication timing of the region assuming a passive movement of the replication fork from the early to the late region. The numbers next to the dashed lines represent the RMSD values between the dots and the dashed line. Note the good agreement between the predicted passive replication time (dashed line) and the actual timing (black dots).

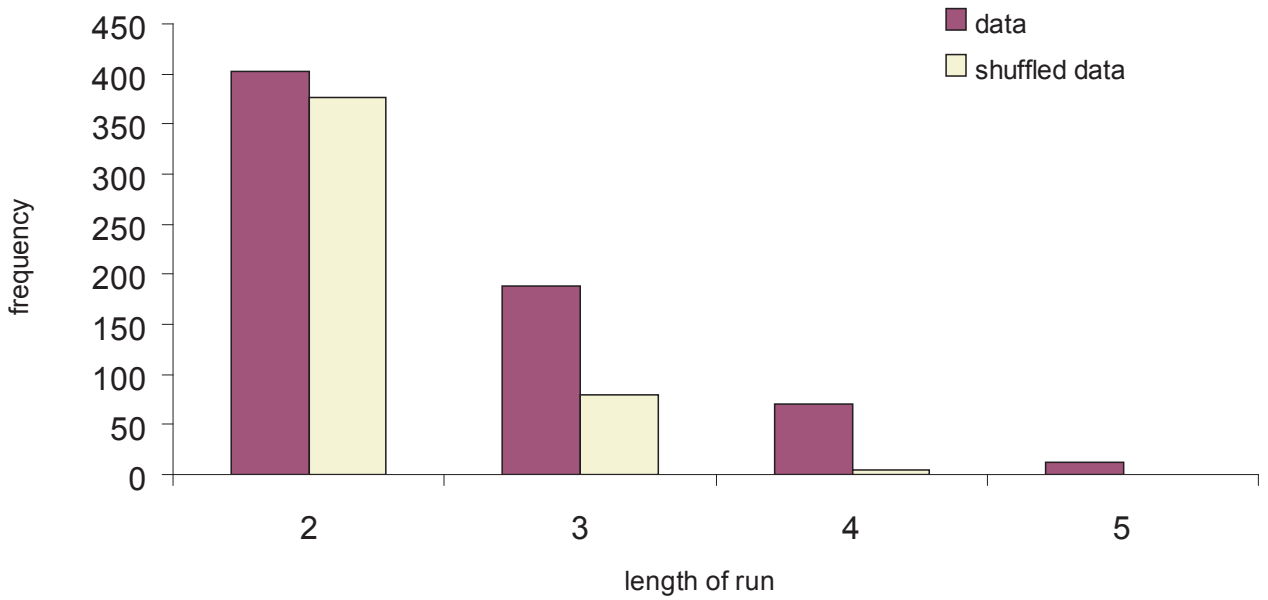

Figure S9 Runs length analysis
In order to evaluate the significance of the gradual replication zones in our data, the length of each run of consecutive replication zones was calculated (i.e. a run with replication zones 7,6 and 5 was considered as a run with a length of 2) . Longer runs were significantly enriched in our data (red) compared to the shuffled data (yellow) (p-value $5*10^{-43}$, t-test).

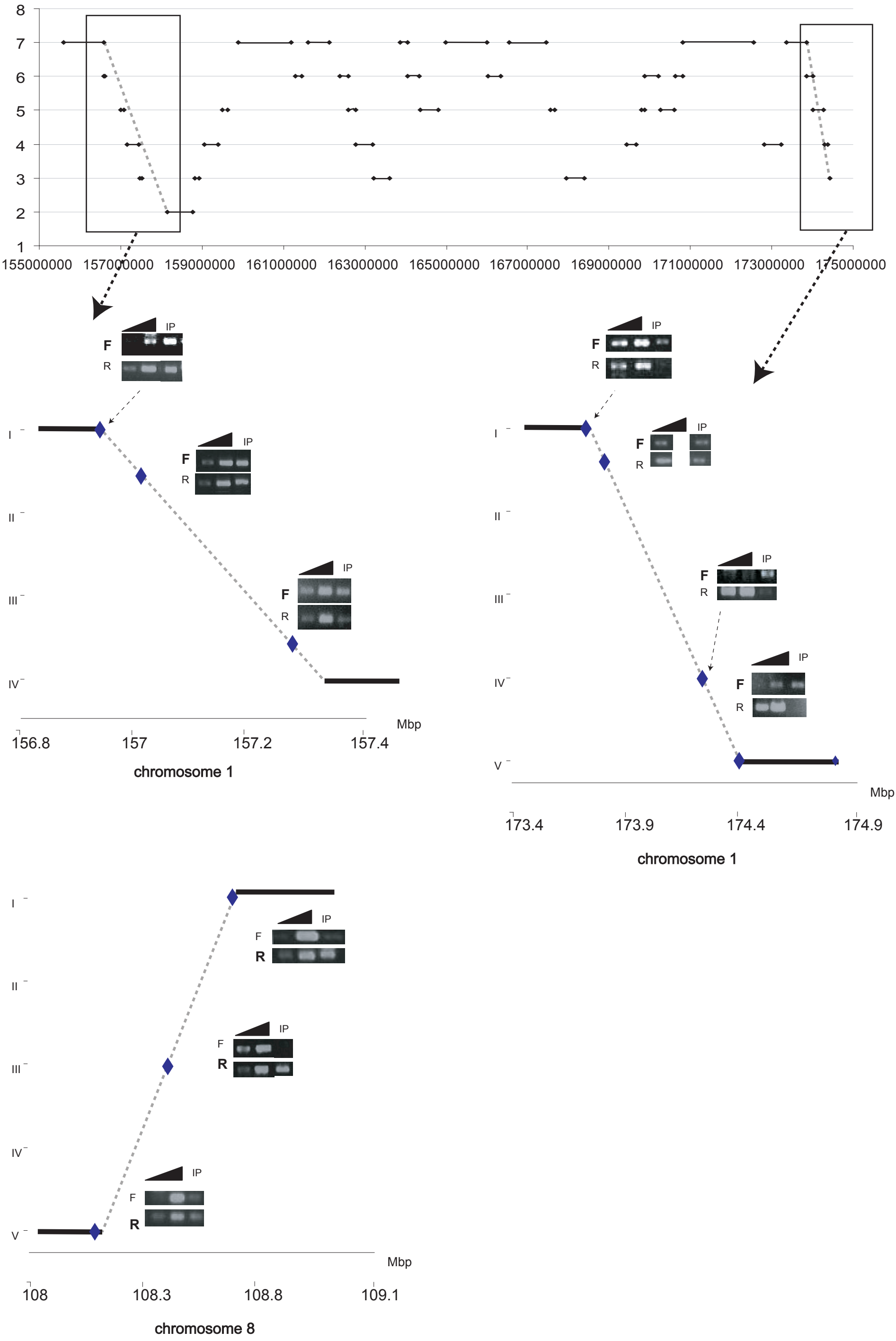

Figure S10 Replication fork direction analysis.
Three regions were analyzed for replication fork direction (using the method described in Fig4c). Note that all primer sets assayed in each region show the same direction of the fork (marked in bold letters) strongly suggesting that this entire region is replicated by a single fork.

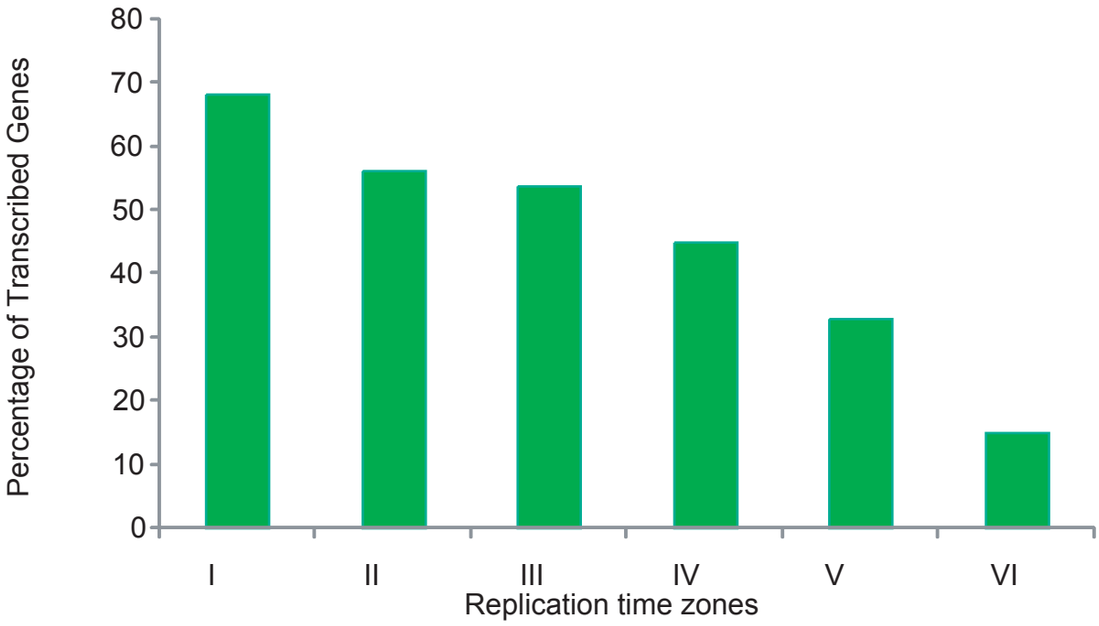

Figure S11 Correlation between replication timing and transcription.
The transcription levels of all genes in L1210 cells were measured using affymetrix 430A 2.0 microarray. The percentage of transcribed genes (annotated as present by the MAS5 algorithm) in each time of replication category is shown. Note that although there is a good correlation between early replication and transcription, the association is more complex, late genes can also be transcribed, whereas not all early genes are transcribed.

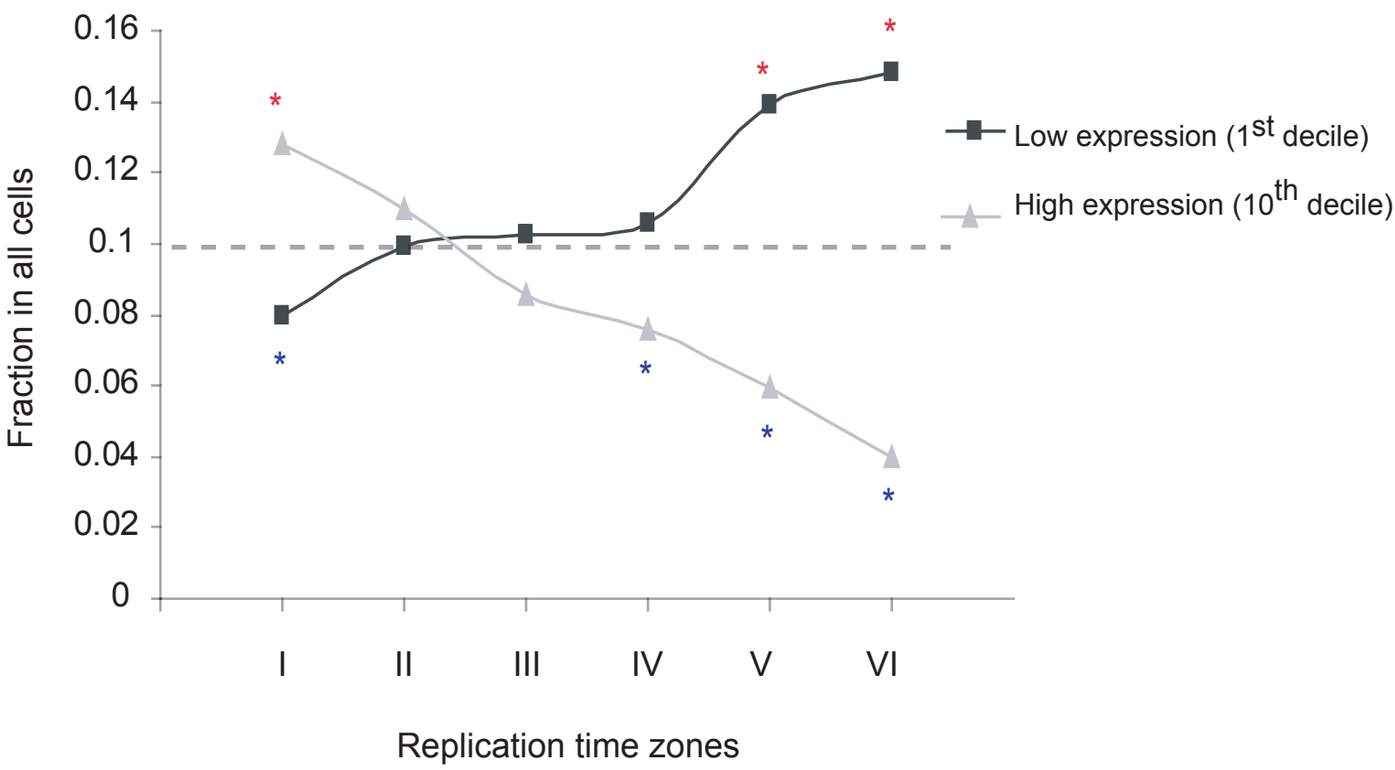

Figure S12 Correspondence between replication timing and average transcript level
The average expression data in 61 mouse tissues (Su et al., 2004) were divided into ten deciles. The percentage of genes in each replication time zone which fall into the 1st and 10th expression deciles is shown. Significant (P<0.0005) enrichment or depletion over the expected value of 10% (dashed horizontal line) is marked by asterisks. Early clusters are enriched with highly expressed genes (10th decile) and depleted with low expressed genes (1st decile) while late clusters show the opposite pattern. Note that this correlation exists even though the expression levels are derived from a large variety of tissues and not from lymphocytes alone. This observation supports the idea that replication timing correlates with the transcription potential rather than with the actual transcription.

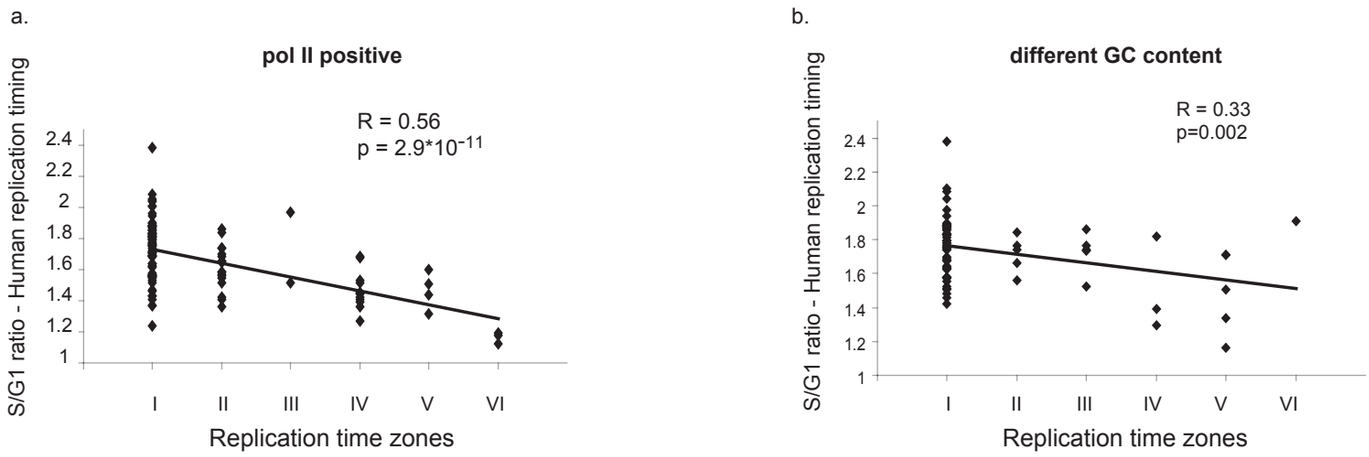

Figure S13 Conservation in replication timing between human and mouse
Correlation between human and mouse replication time was analyzed for genes which are expressed (a) and for genes that their GC content environment has changed between human and mouse (b). A change in the GC content environment was defined by ranking all the genes in each organism according to their GC content environment. Each ranked list was divided into three categories (high, middle and low GC content) each containing third of the genes. Genes that were assigned to different categories in the two organisms were defined as having a different GC content. The human replication time is shown as S:G1 ratio values (Woodfine et al., Human Molecular Genetics, 2004) in which higher values correspond to early replication. The regression line is shown together with its R and F statistics P values.

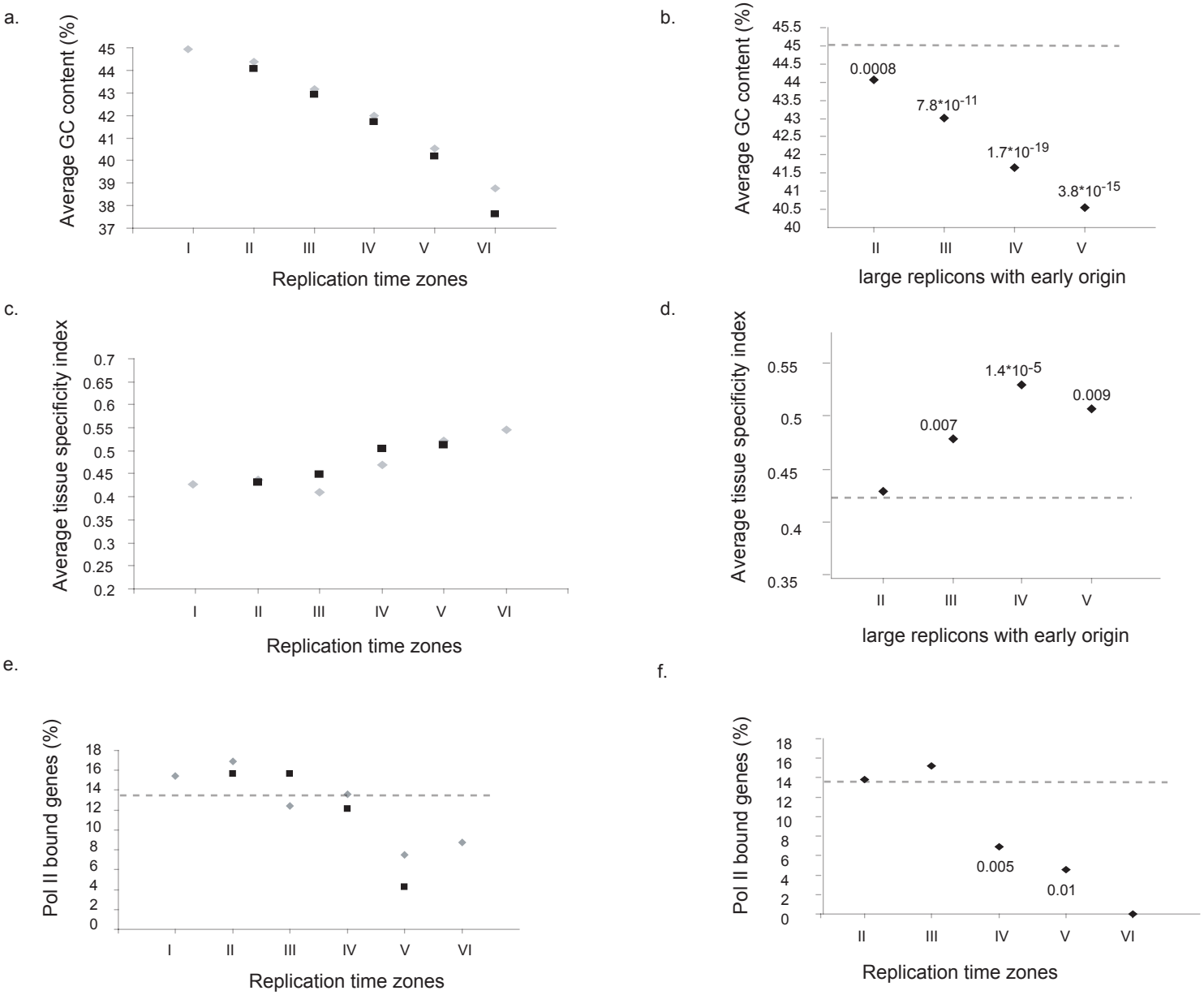

Figure S14 Comparison between large replicons and replication time zones

In order to compare the characters of regions that contain origins (grey diamonds in a,c,e) with regions in which replication occurs through the activation of distant origin (black squares in a,c,e), we divided the genome into large replicons and replication time zones. Note that an early replicating region must contain an origin (see methods). a. GC content in each replication time (I-VI) for the two types of replication organization. Note that the two patterns do not differ (p=0.26; t test) from each other. b. Regions that their replication originates at cluster I (early S) were analyzed for the correlation between GC content and time of replication. The dashed line marks the GC content of early replicating regions (cluster I) and thus represents the expected results if the time of origin activation was in correlation with GC content. The average GC content in each point is significantly different from the GC content of the origin (dashed line; t test p values are shown). Moreover, the correlation between the ToR and the GC content exists also for these regions ($R=0.28$, $P<10^{-10}$). c. Average tissue specificity index in each replication time (I-VI) . Again, the two patterns do not differ (p=0.39; t test) from each other. d. Regions that their replication originates at cluster I (early S) were analyzed for the correlation between tissue specificity index and ToR. The average tissue specificity index for each point is significantly different from that of the origin (dashed line; t test p values are shown). Here also, the correlation between the time of replication and the tissue specificity index exists also for these regions ($R=0.15$, $P<10^{-3}$). e. The percentage of RNA Polymerase II bound genes in each replication time (I-VI). Note that the two patterns do not differ (p=0.45, t test) from each other. f. Regions that their replication originates at cluster I (early S) were analyzed for the correlation between RNA polymerase II binding and ToR. p-values (Fisher-exact test) are shown where the percentage of RNA polymerase II bound genes in the replication time zone is significantly different from that of the origin.

a.

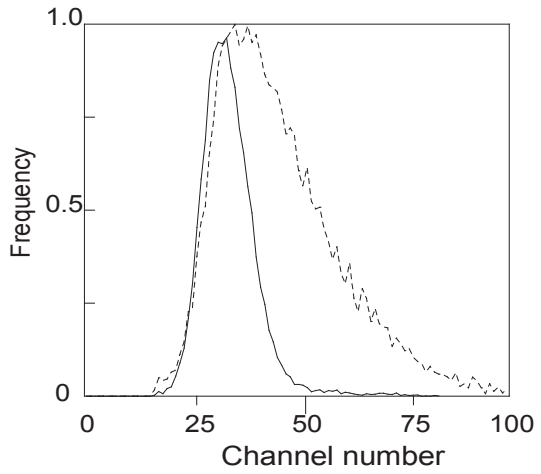

b.

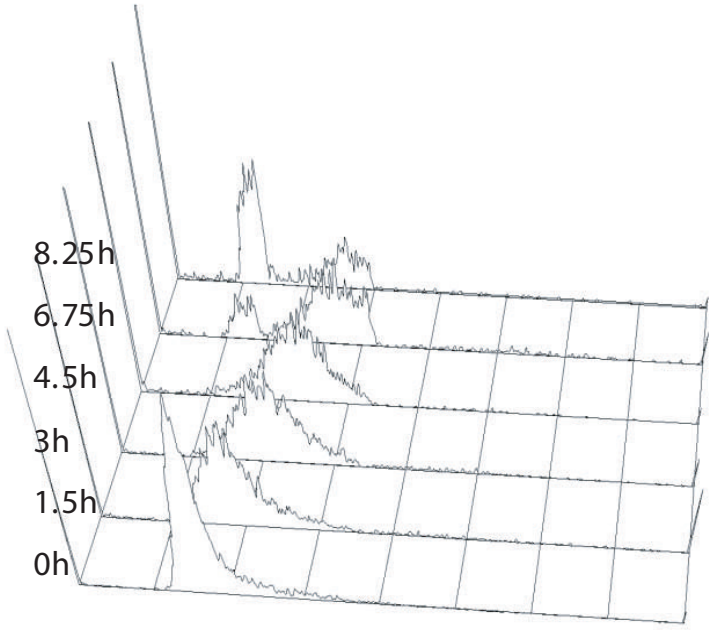

Figure S15 baby machine synchronization

a. Synchronization of the cells isolated from the baby machine was assessed using a ZB Coulter electronic particle counter. The distributions of cell sizes of cells from unsynchronized culture (dashed line) and of newborn cells collected between 3 and 3.75 hours of elution from the baby machine (black line) are shown. Note that essentially all the newborn cells are small (low channel number). b. In order to further asses the synchrony and homogenous population of mitotic cells that were collected from the "Baby machine" samples of mitotic cells were collected for 45 minutes, incubated for the indicated times and analyzed with PI using flow cytometry. Note that the cells are collected at the beginning of the cell cycle (G1) and grow synchronously for about 8h.

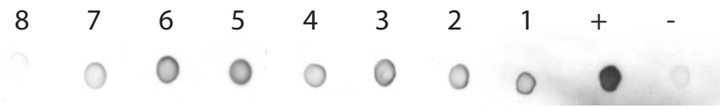

Figure S16 Assessment of BrdU incorporation
Assessment of the amount of BrdU incorporated in each sample was done using a dot blot based technique (see methods). Note that samples 1-6 in which the cells were exposed to the BrdU treatment during S phase (see figure 1a) contain similar amounts of BrdU (sample 7 contains low amount of BrdU since it represents cells exposed to BrdU very late in S phase and possible in early G2 phase). On the other hand sample 8 in which the cells were exposed to BrdU in the G2 phase contains almost no BrdU. The sample denoted by '+' is a positive control (10 hours labeling of BrdU) and the sample detonated by '-' is a negative control. Based on the low amount of BrdU incorporation in sample 8, it was excluded from further experiments. DNA from each sample was measured using the NanoDrop and equal amount of DNA was loaded for each sample.

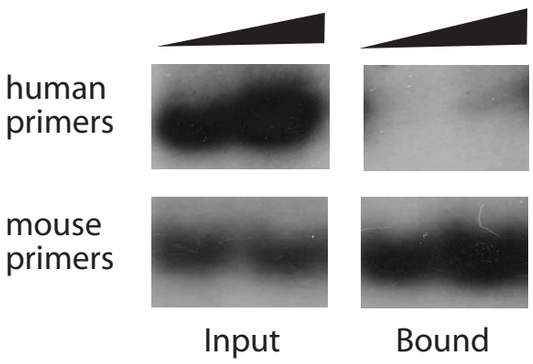

Figure S17 Assessment of BrdU immunoprecipitation specificity.
The specificity of the immunoprecipitation was assessed by mixing BrdU labeled mouse DNA (from L1210 cells) with 6 fold excess of unlabeled human DNA (from K562 cells). After immunoprecipitation the amount of mouse and human DNA was measured by semi quantitative PCR using species specific primers (see primers table). Note that almost no human DNA was detected after the immunoprecipitation (bound) whereas in the input samples it was in excess.

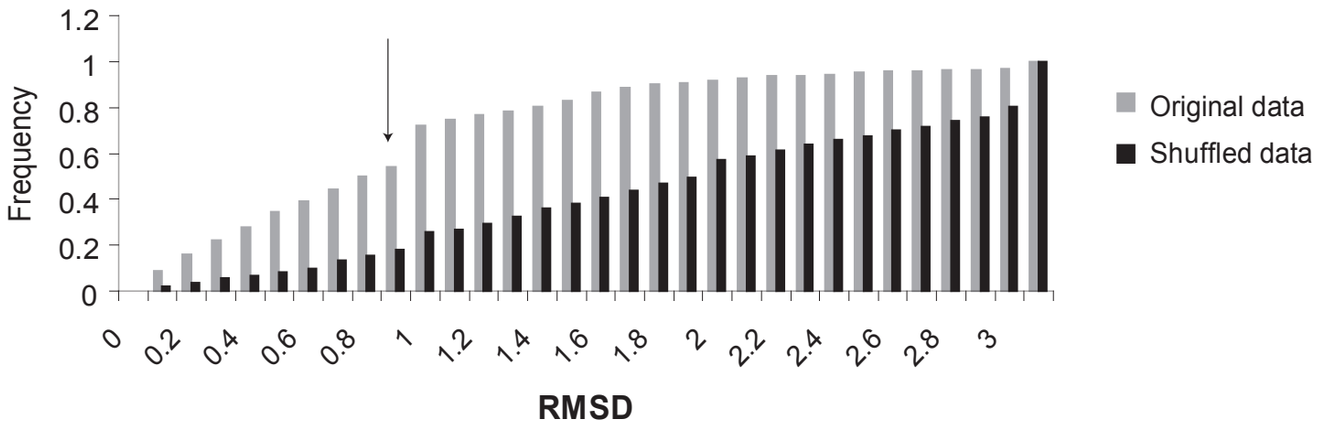

Figure S18 Effect of shuffling the data on passive replication zones identification
The root mean square deviation (RMSD) between the replication time of all the short (<250Kb) segments falling between two long segments and the predicted replication time (see figure 4a) was calculated. Cumulative histogram of the RMSD values is shown for the original (grey) and the shuffled (black) data. The arrow marks the threshold chosen for further analysis of passive replication zones (RMSD<1).Note that the RMSD values are lower in the original data than in the shuffled data. For example 54% of the passive zones have RMSD<1 in the original data whereas only 18% (3 fold enrichment) after shuffling.

References

1. Thornton, M.; Eward, K. L.; Helmstetter, C. E., Production of minimally disturbed synchronous cultures of hematopoietic cells. *Biotechniques* **2002,** 32, (5), 1098-100, 1102, 1105.
2. Ueda, J.; Saito, H.; Watanabe, H.; Evers, B. M., Novel and quantitative DNA dot-blotting method for assessment of in vivo proliferation. *Am J Physiol Gastrointest Liver Physiol* **2005,** 288, (4), G842-7.
3. Azuara, V.; Brown, K. E.; Williams, R. R.; Webb, N.; Dillon, N.; Festenstein, R.; Buckle, V.; Merkenschlager, M.; Fisher, A. G., Heritable gene silencing in lymphocytes delays chromatid resolution without affecting the timing of DNA replication. *Nat Cell Biol* **2003,** 5, (7), 668-74.
4. Kitsberg, D.; Selig, S.; Brandeis, M.; Simon, I.; Keshet, I.; Driscoll, D. J.; Nicholls, R. D.; Cedar, H., Allele-specific replication timing of imprinted gene regions. *Nature* **1993,** 364, (6436), 459-63.
5. Selig, S.; Okumura, K.; Ward, D. C.; Cedar, H., Delineation of DNA replication time zones by fluorescence in situ hybridization. *Embo J* **1992,** 11, (3), 1217-25.
6. Goren, A.; Tabib, A.; Hecht, M.; Cedar, H., DNA replication timing of the human {beta}-globin domain is controlled by histone modification at the origin. *Genes Dev* **2008,** 22, (10), 1319-24.
7. Lieb, J. D.; Liu, X.; Botstein, D.; Brown, P. O., Promoter-specific binding of Rap1 revealed by genome-wide maps of protein-DNA association. *Nat Genet* **2001,** 28, (4), 327-34.
8. Odom, D. T.; Zizlsperger, N.; Gordon, D. B.; Bell, G. W.; Rinaldi, N. J.; Murray, H. L.; Volkert, T. L.; Schreiber, J.; Rolfe, P. A.; Gifford, D. K.; Fraenkel, E.; Bell, G. I.; Young, R. A., Control of pancreas and liver gene expression by HNF transcription factors. *Science* **2004,** 303, (5662), 1378-81.
9. http://cmgm.stanford.edu/pbrown/protocols/index.html.
10. Yanai, I.; Benjamin, H.; Shmoish, M.; Chalifa-Caspi, V.; Shklar, M.; Ophir, R.; Bar-Even, A.; Horn-Saban, S.; Safran, M.; Domany, E.; Lancet, D.; Shmueli, O., Genome-wide midrange transcription profiles reveal expression level relationships in human tissue specification. *Bioinformatics* **2005,** 21, (5), 650-9.
11. Su, A. I.; Wiltshire, T.; Batalov, S.; Lapp, H.; Ching, K. A.; Block, D.; Zhang, J.; Soden, R.; Hayakawa, M.; Kreiman, G.; Cooke, M. P.; Walker, J. R.; Hogenesch, J. B., A gene atlas of the mouse and human protein-encoding transcriptomes. *Proc Natl Acad Sci U S A* **2004,** 101, (16), 6062-7.
12. Woodfine, K.; Fiegler, H.; Beare, D. M.; Collins, J. E.; McCann, O. T.; Young, B. D.; Debernardi, S.; Mott, R.; Dunham, I.; Carter, N. P., Replication timing of the human genome. *Hum Mol Genet* **2004,** 13, (2), 191-202.
13. Ernst, J.; Bar-Joseph, Z., STEM: a tool for the analysis of short time series gene expression data. *BMC Bioinformatics* **2006,** 7, 191.
14. Hatton, K. S.; Dhar, V.; Brown, E. H.; Iqbal, M. A.; Stuart, S.; Didamo, V. T.; Schildkraut, C. L., Replication program of active and inactive multigene families in mammalian cells. *Mol Cell Biol* **1988,** 8, (5), 2149-58.
15. Azuara, V.; Perry, P.; Sauer, S.; Spivakov, M.; Jorgensen, H. F.; John, R. M.; Gouti, M.; Casanova, M.; Warnes, G.; Merkenschlager, M.; Fisher, A. G., Chromatin signatures of pluripotent cell lines. *Nat Cell Biol* **2006,** 8, (5), 532-8.

16. Hiratani, I.; Leskovar, A.; Gilbert, D. M., Differentiation-induced replication-timing changes are restricted to AT-rich/long interspersed nuclear element (LINE)-rich isochores. *Proc Natl Acad Sci U S A* **2004,** 101, (48), 16861-6.